Icarus 203 (2009) 58–65

Contents lists available at ScienceDirect

Icarus

journal homepage: www.elsevier.com/locate/icarus

Evidence for Mg-rich carbonates on Mars from a 3.9 μm absorption feature

Ernesto Palomba [a,*], Angelo Zinzi [a,b], Edward A. Cloutis [c], Mario D'Amore [a], Davide Grassi [a], Alessandro Maturilli [d]

[a] INAF – Istituto di Fisica dello Spazio Interplanetario, via del Fosso del Cavaliere, 100, 00133 Roma, Italy
[b] Dipartimento di Fisica, Università di L'Aquila, Via Vetoio, Coppito, AQ, Italy
[c] University of Winnipeg, 515 Portage Avenue, Winnipeg, Man., Canada
[d] Institute of Planetary Research, DLR, Rutherfordstrasse 2, 12489 Berlin, Germany

ARTICLE INFO

Article history:
Received 11 August 2008
Revised 15 April 2009
Accepted 24 April 2009
Available online 9 May 2009

Keywords:
Infrared observations
Mars
Mars, atmosphere
Mars, surface
Mineralogy

ABSTRACT

The origin and nature of the early atmosphere of Mars is still debated. The discovery of sulfate deposits on the surface, coupled with the evidence that there are not large abundances of carbonates detectable on Mars in the optically accessible part of the regolith, leaves open different paleoclimatic evolutionary pathways. Even if carbonates are responsible for the feature observed by TES and Mini-TES at 6.76 μm, alternative hypotheses suggest that it could be due to the presence of Hydrated Iron Sulfates (HIS). Carbonates can be discerned from HIS by investigating the spectral region in which a strong overtone carbonate band is present. The Planetary Fourier Spectrometer on board the Mars Express spacecraft has acquired several thousand martian spectra in the range 1.2–45 μm since January 2004, most of which show a weak absorption feature between 3.8 and 4 μm. A similar feature was observed previously from the Earth, but its origin could not be straightforwardly ascribed to surface materials, and specifically to carbonates. Here we show the surficial nature of this band that can be ascribed to carbonate mixed with the martian soil materials. The materials that best reproduce the detected feature are Mg-rich carbonates (huntite [$CaMg_3(CO_3)_4$] and/or magnesite [$MgCO_3$]). The presence of carbonates is demonstrated in both bright and dark martian regions. An evaluation of the likeliest abundance gives an upper limit of ~10 wt%. The widespread distribution of carbonates supports scenarios that suggest carbonate formation occurred not by precipitation in a water-rich environment but by weathering processes.

1. Introduction

The composition and evolution of the early martian atmosphere are still open issues. In particular the role played by CO_2 and the other greenhouse gases (e.g., SO_2) is not well understood (Halevy et al., 2007). In order to better constrain plausible atmospheric evolutionary pathways (Bullock and Moore, 2007; Chevrier et al., 2007) a rigorous search for minerals that could have originated by the interaction of these compounds with the surface is necessary. One of the key mineral groups that can be used as a tracer of atmospheric evolution is carbonates. Until recently, clear identification of carbonate minerals on the martian surface has not been achieved, although thermal IR observations have strongly suggested the presence of low concentrations of carbonates in the surficial or airborne dust (Bandfield et al., 2000, 2003). Most recently, Mg-carbonates have been detected in lithified deposits and eroded topography in the Nili Fossae region (Ehlmann et al., 2008).

The search for carbonates on Mars can be performed at infrared (IR) wavelengths because carbonates have several characteristic spectral features in this spectral range: their v_2, v_3 and v_4 fundamental bands are located, respectively, near 11.2, 6.5 and 13.7 μm, while the overtone and combination bands are located near 2.35, 2.55, and 4.0 μm (Farmer, 1974; Salisbury, 1991; Gaffey et al., 1993; Calvin et al., 1994; Lane and Christensen, 1997). From the perspective of remote sensing detection of carbonates on Mars, the v_4 band is located on the wing of the strong 16 μm CO_2 band, while the v_2 band lies in the same wavelength as a strong silicate absorption (dust and surface) feature. Moreover, both the v_2 and v_4 bands are weak; therefore, the v_3 band is the only readily detectable fundamental band.

Several observations in the IR have been undertaken to detect carbonates on Mars. Spectra obtained for the full martian disk, or at very low spatial resolutions, provided possible detections of a spectral feature around 6.7 μm, which was tentatively assigned to carbonates in atmospheric dust (Pollack et al., 1990). The overtone bands at 2.35 and 2.55 μm, with band depth of a few percent, were detected independently by two Earth-based observations and tentatively assigned to carbonate anions (Bell et al., 1994; Lellouch et al., 2000). Finally, Blaney and McCord (1989) detected a 4 μm band attributed to surface carbonate, although no atmospheric correction was performed to obtain the real surface component.

* Corresponding author. Fax: +39 6 4993 4383.
E-mail address: ernesto.palomba@ifsi-roma.inaf.it (E. Palomba).

0019-1035/$ - see front matter © 2009 Elsevier Inc. All rights reserved.
doi:10.1016/j.icarus.2009.04.013

Ehlmann et al. (2008), by using the orbiting CRISM instrument onboard MRO, identified lithified and eroded deposits of Mg-carbonate in the Nili Fossae region on the basis of diagnostic absorption bands in the 2.3-, 2.5- and 4-μm regions.

TES observations of high-albedo regions and Mini-TES analysis of the Gusev Crater area showed a clear and complex spectral structure with two emissivity minima at 6.33 and 7.19 μm (1580 and 1390 cm^{-1}) that were attributed to the strong spectral influence that the ν_3 carbonate band has on the volume scattering component of the relatively non-absorbing basaltic matrix in the observed spectra (Bandfield et al., 2003; Christensen et al., 2004). The study of this spectral behavior suggested an upper limit of 5% by weight of carbonates in the high-albedo regions of the martian surface. Since the low-albedo regions are formed by coarser particles, in which the surface scattering component prevails over the volume scattering component, the complex structure discussed above is absent. However, the usual technique that is used to extract compositional information in these regions (i.e., linear deconvolution) did not show evidence of carbonate, providing an upper limit of 10–15 wt.% (Christensen et al., 2000).

More recent observations by the OMEGA spectrometer on board the Mars Express mission, while showing extensive deposits of sulfates and hydrated minerals, have not yet provided evidence of carbonates on the martian surface (Bibring et al., 2005), encouraging the authors to hypothesize an ancient martian atmosphere not favorable to carbonate formation (Chevrier et al., 2007).

The OMEGA "non-detection" could have been either due to the absence of carbonate on the surface or the weakness of the carbonate overtone bands relative to the sulfate bands in the spectral region investigated by OMEGA ($\lambda < 2.5$ μm). The apparent absence of carbonates could be explained by the alternative presence of Hydrous Iron Sulfates (HIS e.g., ferricopiapite and rozenite), whose spectral characteristics fit very well the observed TES and Mini-TES feature centered at 6.76 μm (1480 cm^{-1}), similar to carbonates (Lane et al., 2004). It is worth noting that, in contrast to carbonates, HIS generally do not display strong overtone features at 4 μm (Bishop et al., 2006; Cloutis et al., 2006). Therefore, a clear detection of carbonates on Mars can be fruitfully performed by analyzing this spectral range, and to this end we used Mars Express Planetary Fourier Spectrometer (MEX-PFS) data, focusing our analysis on data centered at 4 μm.

2. PFS data selection

The Planetary Fourier Spectrometer (PFS) on board the European Space Agency/Mars Express mission (Formisano et al., 2005), operating since January 2004, is an infrared spectrometer covering the spectral range from 1.2 to 45 μm (with a single footprint at periapsis about 10 km wide) by means of two spectral channels: the short wavelength one (SW) operates between 1.2 and 5.5 μm (8190–1820 cm^{-1}) (Giuranna et al., 2005a) and the long wavelength (LW) channel spans from 5.5 to 45 μm (1820–220 cm^{-1}) (Giuranna et al., 2005b) (both with a spectral resolution of 1.3 cm^{-1}). Due to its configuration, the SW and LW channels acquire spectra of the same field of view at the same time.

We analyzed two sets of data, one from low-albedo regions (TES albedo < 0.20) and one from high-albedo regions (TES albedo > 0.25). The low-albedo regions included Syrtis Major, Margaritifer Terra, Terra Cimmeria and Acidalia Planitia, and the high-albedo regions included Elysium Planitia and Lunae Planum. Spectra acquired over Syrtis Major were grouped spatially into three subsets: East, Northwest and Southwest.

All the spectra analyzed in this work were acquired in nadir mode, i.e., in conditions where the air column between spacecraft and surface is minimum. A typical spectrum acquired over regions with low surface temperature (e.g., 210 K) has a Signal-to-Noise Ratio (SNR) of 10 (Giuranna et al., 2005a). In order to improve this value, we averaged up to 80 SW spectra for each orbit; similar spectral averaging was performed by Ehlmann et al. (2008) on CRISM data to also improve SNR. As a consequence, the corresponding footprint for a single averaged spectrum is elongated and covers several thousand square kilometers (as shown in Fig. 1) and a typical averaged spectrum has a SNR around 100, allowing us to discern band depths down to 1%.

3. Data analysis

By examining the PFS-SW averaged spectra we discerned an absorption feature centered around 3.8–4 μm. This feature is present in nearly all the examined spectra, being absent only in small areas inside Acidalia Planitia and Terra Cimmeria. We attribute this feature to carbonates present in the martian surface. Its intermittent nature is not unexpected if it is associated with the regolith and not the suspended dust. It is likely that the carbonate may be associated with both surface components and dust, as carbonates appear to be present in both lithified deposits and eroded terrains (Ehlmann et al., 2008). It is not possible to specify to what proportions the carbonates are associated with bedrock or windblown dust, but the fact that the carbonates are widespread and where absent, are absent only in dark regions (Acidalia Planitia and Terra Cimmeria), favors a windblown origin.

The portion of the infrared spectrum that we studied (centered around 3.9 μm) lacks strong atmospheric features. However, since the observed band is weak, the degree of atmospheric contribution must be evaluated; the main contribution being the CO_2 isotopic bands, occurring at 4.00, 3.83, 3.63 μm (see Fig. 2, plot A). In addition, solar lines (Fiorenza and Formisano, 2005) give a non-negligible, constant contribution to the observed spectrum in this wavelength interval (Smith and Gottlieb, 1974). Due to the two-channel instrumental configuration of PFS, we were able to perform an *ad hoc* atmospheric correction for every SW spectrum by computing actual parameters (i.e., surface temperature and temperature profile) with the LW channel data and assuming that surface, atmospheric and solar contributions are multiplicative.

A typical sequence of atmospheric and solar removal methodology (Fig. 2) starts with the normalization of the PFS-SW observed band to a continuum (usually taken as a second order polynomial fit from the wings of the atmospheric band triplet, e.g., at 3.55, 3.69, 4.06 μm). The solar contribution is removed first by ratioing, applying the solar spectrum (B) obtained by Fiorenza and Formisano (2005). The CO_2 isotopic bands can vary in intensity, depending on the local climate. We reproduced this behavior by using a radiative transfer model (Grassi et al., 2005), obtaining a synthetic spectrum (A) that is used to remove the isotopic bands from the observed spectrum (D). In order to account for the real conditions of observation, for each SW average spectrum we used the corresponding LW spectra to extract the actual vertical temperature profiles to be used in the model. Since the CO_2 transmittance synthetic spectrum is obtained for fixed observational geometries (relative to both incidence and emission angle equal to 0°), for each spectrum we derived the proper transmittance of the air column for the actual observational parameters, applying a least square fit algorithm. We finally remove the CO_2 isotopic bands from the observed band by ratioing the synthetic spectrum.

The best fit obtained by using only atmospheric and solar contributions leaves unaccounted for absorption features in the PFS band shape (Fig. 2 – plot E), indicative of the presence of an additional spectral contribution. We attribute this additional spectral component to surface materials. Before considering the surface as being responsible for the 4 μm spectral feature, several other pos-

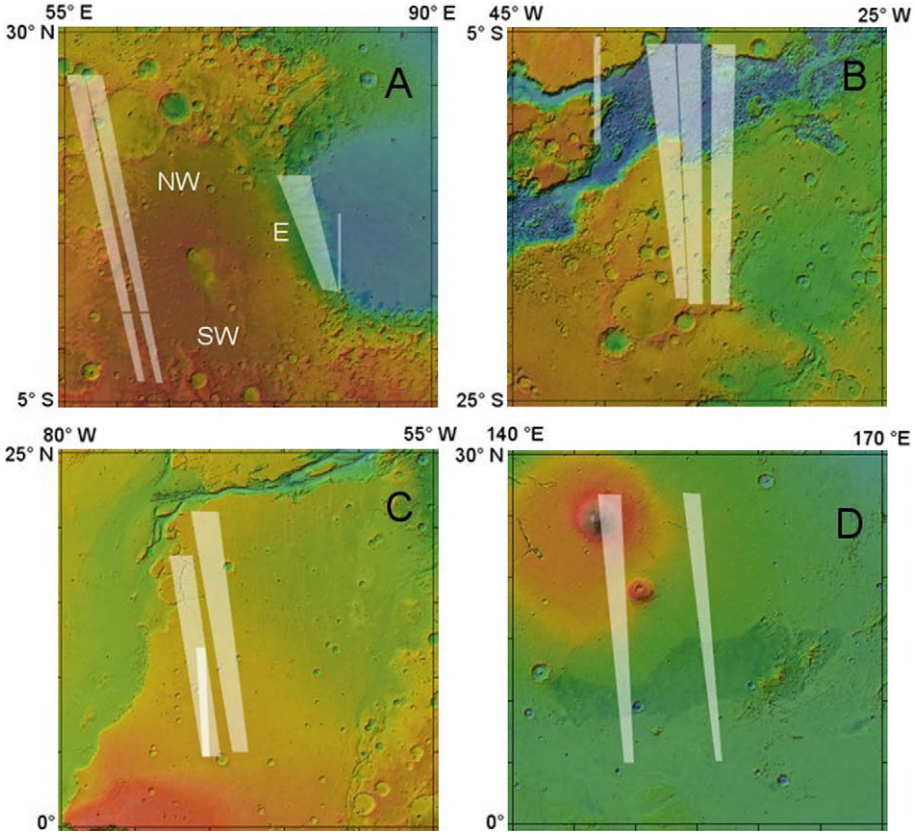

Fig. 1. MOLA color shaded relief (128 ppd) maps of studied regions. (A) Syrtis Major divided into three sub-regions: Northwest (NW), Southwest (SW) and East (E). (B) Margaritifer Terra. (C) Lunae Planum. (D) Elysium. The PFS-SW footprints on the planetary surface are indicated by the white semitransparent strips. The spectra were acquired during the first six months of PFS activity, corresponding to heliocentric longitude Ls 335 to 60 (northern fall to winter, which implies a decrease of the mean surface temperatures in most of the northern hemisphere).

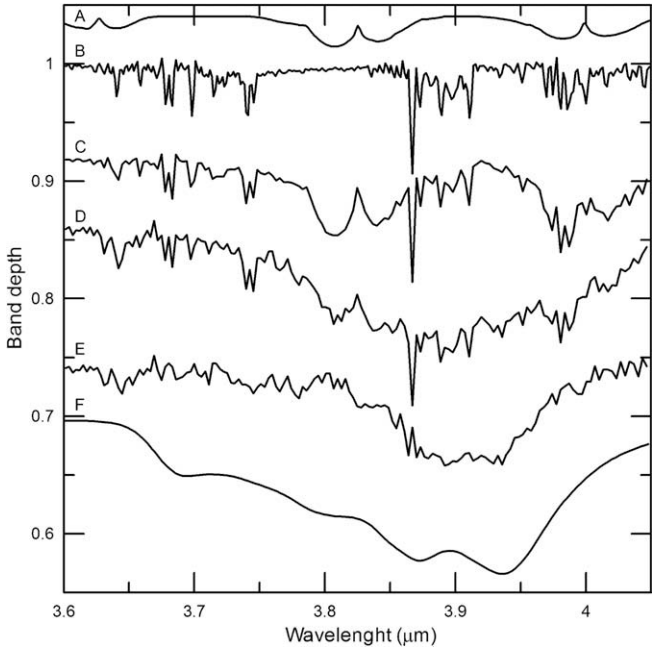

Fig. 2. From top to bottom: (A) atmospheric CO_2 transmittance (as computed by Grassi et al., 2005), (B) solar bands, (C) best fit accounting for the solar and the atmospheric bands, (D) PFS-SW band depth, (E) PFS-SW corrected (ratio) band and (F) bi-directional reflectance laboratory spectra of fine grained (<45 μm) huntite. The weight that the surficial band has on the observed PFS spectra is comparable to one of the atmospheric counterparts, even in different spectral intervals, as shown by the third, fourth and fifth spectra from the top.

sible processes (e.g., dust in the atmosphere, instrumental effects and residual atmospheric bands) were considered. A more detailed discussion of atmospheric dust is needed, since it is a permanent and important component of the martian environment. Suspended dust adds a transmittance contribution to the spectrum introducing, possibly, only a spectral slope (Erard, 2001) The stretching and bending vibration bands of common planetary materials occur between 8.5 and 40 μm (Hunt, 1982), while the 4 μm spectral region is populated by overtone and combination bands. The absorption coefficients of these bands are several times weaker than the corresponding fundamentals. Therefore, the detection of overtones in transmittance is possible only for minerals present in large quantities and during periods of high atmospheric dust opacity. As an example, for limestone the absorption coefficient of the 4 μm overtone band is five times weaker than the v_2 fundamental at 11 μm (Orofino et al., 1998). A simulation of martian spectra for dust optical depth (τ) = 0.2, with a dust composed of palagonite (85 wt.%) and limestone (15 wt.%) produces a 2% deep band at 11 μm, and a smaller band depth for the overtone (Orofino et al., 1998). Definitive evidence that the atmospheric dust loading cannot be responsible for the observed feature is obtained by analyzing the behavior of the 3.9 μm band depth vs the dust optical depth (Fig. 3). Applying the retrieval algorithm described by Grassi et al. (2005), we computed the atmospheric dust loading (integrated τ at 1100 cm^{-1}) from the PFS-LW data. If the 3.9 μm band was due to the atmospheric dust, we should expect band depth to increase with increasing τ, a trend not evident in Fig. 3.

An alternative and more sophisticated approach to understand the surficial origin of the observed spectral feature, ruling out both

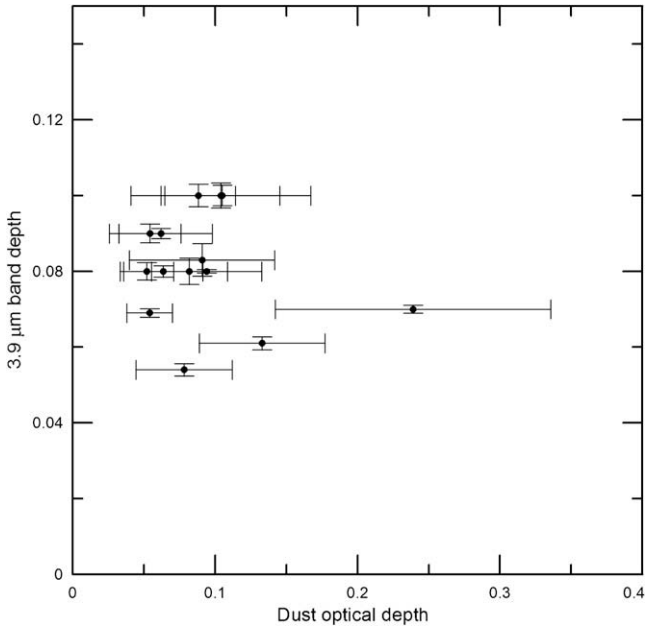

Fig. 3. Variation of band depth at 3.9 μm with dust optical depth. No systematic behavior is present. The bars represent the data standard deviations.

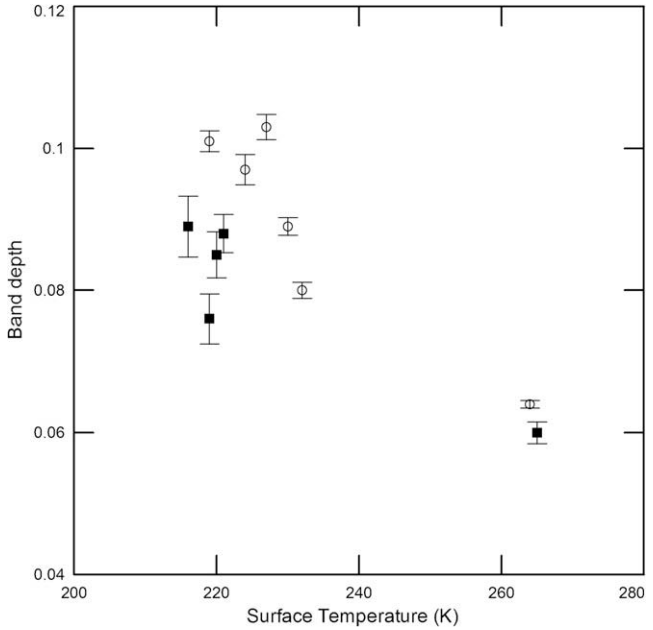

Fig. 4. Band depth vs surface temperature for Syrtis (circles) and Margaritifer (squares) regions. The vertical bars represent the band depth standard deviation. The temperature uncertainty is estimated to be near 5 K. The band depth behavior with respect to surface temperature is clearly evident, demonstrating the surface origin of the band.

instrumental and residual atmospheric effects, is based upon the thermal properties of the martian surface in the investigated spectral region. Since in the 3–5 μm interval the radiance from Mars consists of thermal emitted and solar reflected radiation contributions, their relative weights change dramatically with surface temperature and albedo; e.g., at 4 μm for dark regions (with a typical reflectance factor at 4 μm of 0.18 – Erard and Calvin, 1997) the thermal contribution is less than 5% of the total radiation at 225 K, while it reaches 41% at 270 K; conversely for a typical bright region (reflectance factor at 4 μm equal to 0.3 – Erard and Calvin, 1997) the thermal contribution is 2% of the total radiation for $T = 225$ K and 26% at 270 K. Taking this into account, and applying Kirchoff's law to Mars (Salisbury and Wald, 1992) (i.e., emissivity is the complement of reflectivity), troughs in reflection would appear as peaks in emission. The overall effect is an obliteration of the absorption bands as the two contributions tend to be equivalent. This implies that, in this spectral region, the depth of an absorption feature for a fixed martian area (or for constant albedo) will decrease with increasing surface temperature. This relationship is shown for the atmospherically removed PFS data in Fig. 4, where the 3.9 μm band depths are plotted against the surface temperatures (as obtained from the LW data).

4. Nature of the 3.9-μm region PFS absorption feature

The retrieved surface-related absorption feature displays a similar spectral shape in all the analyzed areas, with the two main absorption features centered near 3.88–3.89 and 3.93 μm (see Table 1). The PFS band along with those of some minerals of planetary interest, are shown in Fig. 5. Of the various candidate minerals examined (see Table 2), only carbonates have similar band positions to the PFS bands, whereas minerals belonging to other classes almost always have bands located at least 50 nm from the PFS bands (Fig. 6). A few do have one or two bands within 50 nm of the PFS bands, including sodium nitrite (3.78 and 3.98 μm), sodium nitrate (4.03 and 4.09 μm), potassium nitrate (4.03 and 4.12 μm), coquimbite (a single shallow band at 4.00 μm, about 4% deep), and the phosphate apatite (with a single shallow band at 3.97 μm about 2% deep). However, these materials

Table 1
PFS surface band. Location of the two band minima and TES albedo relative to each studied region on Mars.

Region	Band I position	Band II position	TES Albedo
Syrtis East	3.88	3.93	0.18
Syrtis Northwest	3.89	3.93	0.14
Syrtis Southwest	3.88	3.93	0.13
Margaritifer	3.89	3.94	0.14
Lunae Planum	3.89	3.93	0.24
Elysium	3.89	–	0.26

either do not display two absorption bands close to the PFS values or exhibit additional absorption bands not seen in the PFS spectra (Fig. 5). We also examined bicarbonate minerals (nahcolite and trona) and scapolites (generally metamorphic/metasomatic CO_3- and SO_4-bearing alumino-silicates (Deer et al., 1966). None of these minerals exhibit absorption bands in the same positions as those seen in the PFS spectra. Thus, it appears that no plausible mineral class other than carbonates can account for the PFS features in the 3.9 μm region.

Of the carbonates, the best candidates are huntite, magnesite, hydromagnesite, northupite, and azurite. Of these, northupite and azurite have a three-band feature with an additional and more intense band at 3.95 and 4.0 μm, respectively, which are not seen in the PFS spectra. Of the remaining carbonates, hydromagnesite is the least likely candidate: its absorption bands are weaker than the PFS surface bands, even for pure hydromagnesite and its spectrum is generally blue-sloped (reflectance declining toward shorter wavelengths). Dehydration of hydromagnesite by heating the sample does however result in its conversion to magnesite and a spectrum that is nearly identical to that of naturally-occurring magnesite. Both huntite and magnesite exhibit their major absorption bands in the same region as the PFS surface spectra, with only minor differences (~10 nm) between them (Figs. 5 and 6). Consequently, huntite and/or magnesite are the best candidate(s), among the minerals that we included in our study, to explain the absorp-

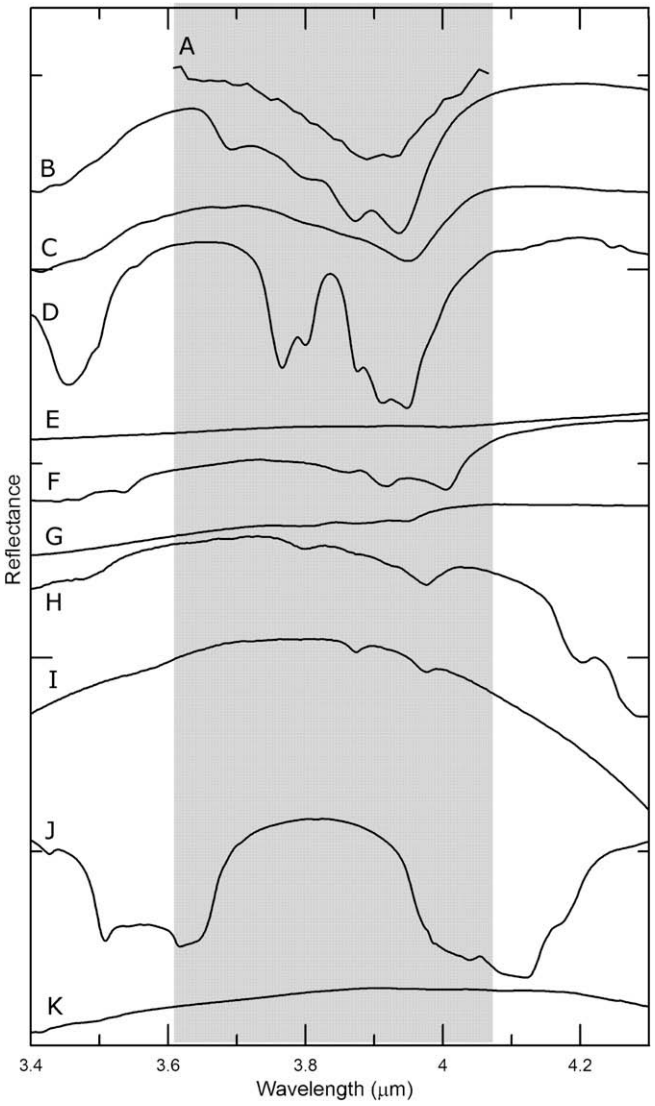

Fig. 5. Spectra of some minerals of planetary interest compared with the PFS absorption feature. From top to bottom: (A) PFS, (B) huntite, (C) magnesite, (D) northupite, (E) coquimbite, (F) azurite, (G) hydromagnesite, (H) anhydrite, (I) gypsum, (J) nitratine, and (K) apatite.

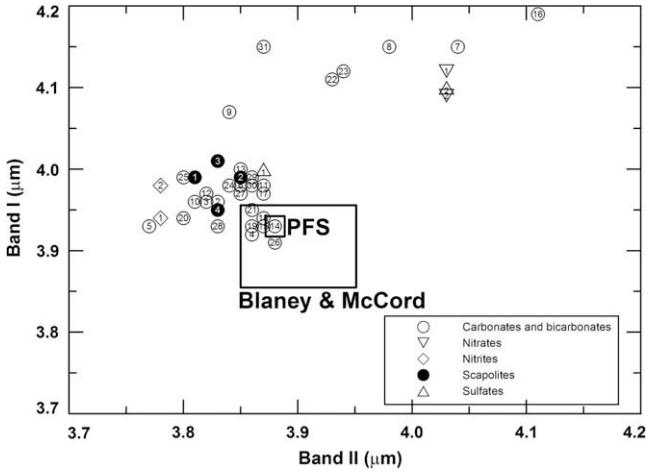

Fig. 6. Wavelength positions of the bands seen in PFS surface spectra and in various minerals (carbonates, bicarbonates, sulfates, nitrites, nitrates, scapolites). The small and large squares give the bands observed by PFS and by Blaney and McCord (1989), respectively. Minerals with very weak bands, as discussed in the text are not shown. The number inside each data point is linked to material specified in Table 2. The Dipyre and Wernerite (scapolites) have the bands in the same position that is displayed in the plot by the scapolite dot number 1.

tion bands in the PFS spectra. The slight spectral variations that exist among the PFS spectra for different regions could suggest the presence of both huntite and magnesite, likely with variations in relative abundances (see Fig. 7). The identification of Mg-rich carbonates as the cause of this feature is consistent with the identification of Mg-rich carbonates as the cause of spectral features in the 2.3-, 2.5-, and 4-μm region of spectra from Nili Fossae (Ehlmann et al., 2008).

If huntite and/or magnesite are indeed present on the martian surface, we can explain the lack of detection of carbonates by the OMEGA spectrometer. The strongest shorter wavelength huntite band is located near 2.49 μm. In pure huntite this band has a depth of 6% (for <45 μm sized particles). By contrast the 3.95 μm band has a depth of up to ~60%, depending on where one constructs the continuum to measure its depth. Therefore, at the abundances of huntite that we have inferred from the PFS data, the 2.49 μm band would be exceedingly weak, and likely not detectable in

Table 2
Minerals used for the determination of the best candidates responsible for the 3.9 μm band. Not listed or shown (for the sake of clarity) is the extensive suite of sulfate spectra from Cloutis et al. (2006) that were also included in the analysis. Nahcolite and trona are bicarbonates.

Carbonates and bicarbonates			
1. Ammonium carbonate	2. Aragonite (with calcite)	3. Aragonite	4. Azurite
5. Brugnatellite	6. Calcite (synthethic)	7. Cerussite (1)	8. Cerussite (2)
9. Dawsonite	10. Dolomite (1)	11. Dolomite (2)	12. Gaspeite
13. Gaylussite	14. Huntite (1)	15. Huntite (2)	16. Hydrocerussite (synthethic)
17. Hydromagnesite (1)	18. Hydromagnesite (2)	19. Hydromagnesite (3)	20. Magnesite (1)
21. Magnesite (2)	22. Malachite (synthetic)	23. Malachite	24. Mn-Calcite
25. Nahcolite	26. Northupite	27. Pirrsonite	28. Shortite
29. Siderite	30. Trona (1)	31. Trona (2)	
Nitrates			
1. Potassium nitrate	2. Sodium nitrate		
Nitrites			
1. $NaNO_2$ (synthetic)	2. Sodium nitrite		
Scapolites			
1. Dipyre	2. Marialite	3. Meionite	4. Mizzonite
5. Wernerite			
Sulfates			
1. Coquimbite	2. Sideronatrite		

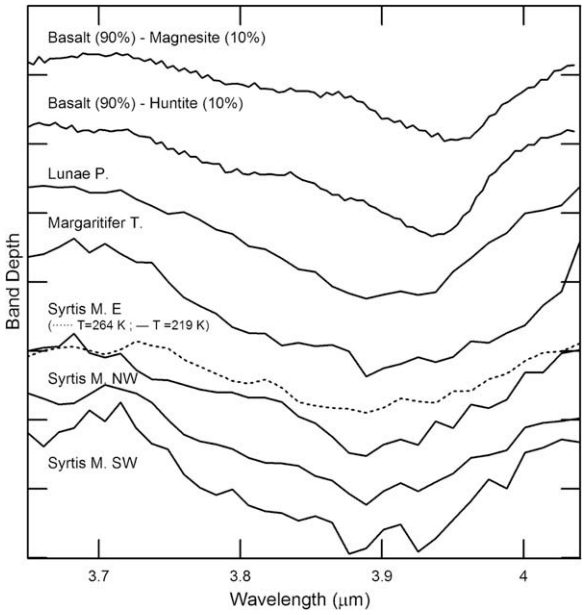

Fig. 7. Comparison between mixtures of basalt and magnesite/huntite and PFS surface spectra of different martian regions. From top to bottom: basalt (90 wt.%) + magnesite (10 wt.%), basalt (90 wt.%) + huntite (10 wt.%), Lunae Planum (orbit 515), Margaritifer Terra (orbit 500), Syrtis Major E (orbit 41) (dotted), Syrtis Major E (orbit 605), Syrtis Major NW and SW (orbit 510). The shown PFS spectra are from cold regions and are all resampled to 8 cm^{-1}. The only warm region (dotted curve) is displayed to show the decrease in band depth due to the thermal radiation (see Section 5). For clarity the spectra are vertically shifted.

OMEGA spectra. Thus, use of the 4-μm region bands provides lower detection limits than shorter wavelength bands.

Magnesite and huntite can form in a variety of geological environments. Of most relevance to Mars, these minerals occur in association with serpentinite as alteration products (Cole and Lancucki, 1975; Stanger and Neal, 1994; Chang et al., 1998; Wilson et al., 2006), as well as in supratidal evaporitic environments (Kinsman, 1967).

5. Discussion

Our study indicates the presence of specific types of carbonates on the martian surface. The band shape and position constrain the cation content (high-Mg) of the carbonate(s). This result also supports the hypothesis that TES and Mini-TES features for moderate to high-albedo regions and Gusev Crater are due to carbonates (Bandfield et al., 2003; Christensen et al., 2004) and not to hydrous iron sulfate (as suggested by Lane et al., 2004), and also supports the detection of similar Mg-rich carbonates in the Nili Fossae region (Ehlmann et al., 2008).

Most notably, these results show that the presence of carbonates is not restricted to the brighter regions but extends to the low-albedo regions of Mars, where the coarse particles forming the regolith prevent the detection at 6.76 μm for abundances lower than 10–15 wt.% (Christensen et al., 2000). The detection of carbonates in both bright and dark regions is consistent with eroded and redistributed carbonates, as seems to be occurring in the Nili Fossae region (Ehlmann et al., 2008). It is worth noting that our Syrtis Major East spectrum, which show the presence of Mg-carbonates, is located just south of the Mg-carbonate exposures in

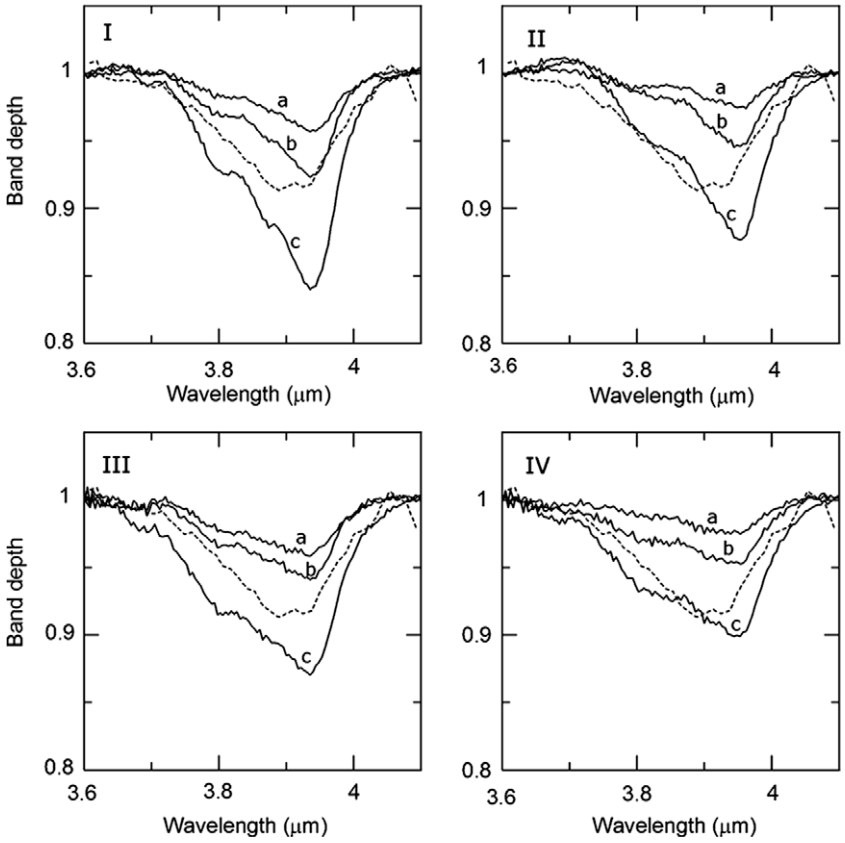

Fig. 8. Band depths of different laboratory mineral mixtures compared with the PFS band shape (Lunae Planum, orbit 515 – dashed line). (I) Basalt + huntite, (II) basalt + magnesite, (III) palagonite + huntite, (IV) palagonite + magnesite. In each plot, carbonate content increases from top to bottom (a) 5 wt.%, (b) 10 wt. %, (c) 20 wt.%.

Table 3
Band widths (FWHM: full width at half maximum) and absolute depths for the various intimate minerals mixtures (all <45 μm grain size) used to model the PFS absorption feature. For the PFS only spectra with surface temperature not larger than 240 K were used.

Mixture (wt.% of end members)	FWHM (μm)	Band depth
Basalt 95–Huntite 5	0.12	0.04
Palagonite 95–Huntite 5	0.19	0.04
Basalt 95–Magnesite 5	0.11	0.03
Palagonite 95–Magnesite 5	0.15	0.03
Basalt 90–Huntite 10	0.12	0.08
Palagonite 90–Huntite 10	0.18	0.06
Basalt 90–Magnesite 10	0.10	0.06
Palagonite 90–Magnesite 10	0.20	0.05
Basalt 80–Muntite 20	0.14	0.16
Palagonite 80–Huntite 20	0.21	0.13
Basalt 80–Magnesite 20	0.13	0.12
Palagonite 80–Magnesite 20	0.22	0.10
PFS 3.9 μm band (cold regions)	0.19 ± 0.03	0.09 ± 0.01

the Nili Fossae region, which also exhibit an absorption feature in the 4-μm region (Ehlmann et al., 2008).

Considering the coldest regions, the absorption feature will represent the solar reflected radiation contribution nearly exclusively and can be used directly to estimate the carbonate abundance. To this aim we acquired reflectance spectra of intimate mixtures (5, 10, and 20 wt.%) of huntite, and magnesite, with either basalt or palagonite, for fine grain sizes (<45 μm). Absorption bands in the 3.9 μm region of the PFS spectra are on the order of 6–10% deep and we found that carbonate abundances of 10 wt.% produce band depths of this magnitude (see Fig. 8). These values are also consistent with expected band depths derived from mixing experiments of carbonates and palagonite (Wagner and Schade, 1996; Fonti et al., 2001). It is worth noting that band depths (and detection limits) will be a function of many factors, including areal vs intimate mixtures, and relative grain sizes (Wagner and Schade, 1996). Thus, our values represent one possible constraint on carbonate abundances.

The PFS spectra have mean full width half maxima (FWHM) of 190 nm, whereas the relative band width of carbonate mixtures vary between 100 and 220. Their FWHM seem to remain almost unchanged with carbonate abundance, while a larger width, closer to the PFS values, is shown by the mixtures containing palagonite (Fig. 8, Table 3). Thus, in both high and low-albedo regions the comparison with laboratory data suggests abundances close to 10% by weight, and more specific measurements are planned to more accurately determine the abundance and distribution of carbonates on the different martian surface units.

The widespread, rather than localized, distribution of carbonates suggests that at least some carbonate formation occurred not by precipitation in a water-rich environment, but only when the hydrologic activity on Mars was ending, as suggested by Bullock and Moore (2007). According to this scenario the martian atmosphere during the late Noachian was made up principally of CO_2, with SO_2 continuously added to the atmosphere by volcanism. A similar environment would have favored the formation of thick sulfate sediments, by maintaining surface temperature above the freezing point of water in an acidic environment (Halevy et al., 2007). At the end of the active volcanism period (i.e., early Hesperian) the atmospheric SO_2 rapidly waned, causing the temperatures to drop below the freezing point of water. The subsequent collapsing of the atmospheric CO_2, coupled with a more alkaline environment, allowed the formation of carbonates in a poorly consolidated form (Bullock and Moore, 2007) that no plausible destructive mechanisms, such as photodissociation, are able to remove (Quinn et al., 2006).

6. Summary

The detection of carbonates, specifically the Mg-rich species huntite and magnesite, across large parts of the martian surface, is consistent with earlier tentative detections of low abundances of carbonates on Mars (e.g., Bandfield et al., 2003), and more recent detections of Mg-rich carbonates (Ehlmann et al., 2008). Our study suggests that the Nili Fossae region is a plausible source region for the more widespread carbonates that we have detected and that once formed, these carbonates are resistant to decomposition (Cloutis et al., 2008).

Acknowledgments

We thank Dr. A. Graps for valuable comments on the manuscript, Dr. A. Terracina for the precious bibliographic work and strong encouragements, Dr. P. Moretti for helpful discussions on the topic, Dr. V. Formisano and the PFS team for their support about the PFS data and related facilities. EAC's work has been supported by grants from the Canadian Space Agency, NSERC, and the University of Winnipeg.

References

Bandfield, J.L., Hamilton, V.E., Christensen, P.R., 2000. A global view of martian surface compositions from MGS-TES. Science 287, 1626–1630.
Bandfield, J.L., Glotch, T.D., Christensen, P.H., 2003. Spectroscopic identification of carbonate minerals in the martian dust. Science 301, 1084–1087.
Bell, J.F., Pollack, J.B., Geballe, T.R., Cruikshank, D.P., Freedman, R., 1994. Spectroscopy of Mars from 2.04 to 2.44 micron during the 1993 opposition: Absolute calibration and atmospheric vs mineralogic origin of narrow absorption features. Icarus 111, 106–123.
Bibring, J.P., and 10 colleagues, 2005. Mars surface diversity as revealed by the OMEGA/Mars Express observations. Science 307, 1576–1581.
Bishop, J.L., Brown, A.J., Parente, M., Lane, M.D., Dyar, M.D., Schiffman, P., Murad, E., Cloutis, E., 2006, VNIR spectra of sulfates formed in solfataric and aqueous acid sulfate environments and applications to Mars. In: Workshop on martian Sulfates as Recorders of Atmospheric-Fluid–Rock Interactions, October 22–24, 2006 in Houston, Texas. LPI Contribution No. 1331, p. 14.
Blaney, D.L., McCord, T.B., 1989. An observational search for carbonates on Mars. J. Geophys. Res. 94, 10159–10166.
Bullock, M.A., Moore, J.M., 2007. Atmospheric conditions on early Mars and the missing layered carbonates. Geophys. Res. Lett. 34. CiteID L19201.
Calvin, W.M., King, T.V., Clark, R.N., 1994. Hydrous carbonates on Mars?: Evidence from Mariner 6/7 infrared spectrometer and ground-based telescopic spectra. J. Geophys. Res. 99 (E7), 14659–14675.
Chang, L.L.Y., Howie, R.A., Zussman, J., 1998. Non-silicates: sulphates, carbonates, phosphates, halides. In: Rock Forming Minerals, vol. 5B. second ed. The Geological Society of London, London. 383 pp.
Chevrier, V., Poulet, F., Bibring, J.-P., 2007. Early geochemical environment of Mars as determined from thermodynamics of phyllosilicates. Nature 448, 60–63.
Christensen, P.R., Bandfield, J.L., Smith, M.D., Hamilton, V.E., Clark, R.N., 2000. Identification of a basaltic component on the martian surface from Thermal Emission Spectrometer data. J. Geophys. Res. 105 (E4), 9609–9621.
Christensen, P.R., and 36 colleagues, 2004. Initial results from the Mini-TES experiment in Gusev Crater from the Spirit rover. Science 305, 837–842.
Cloutis, E.A., Hawthorne, F.C., Mertzman, S.A., Krenn, K., Craig, M.A., Marcino, D., Methot, M., Strong, J., Mustard, J.F., Blaney, D.L., Bell III, J.F., Vilas, F., 2006. Detection and discrimination of sulfate minerals using reflectance spectroscopy. Icarus 184, 121–157.
Cloutis, E.A., Craig, M.A., Kruzelecky, R.V., Jamroz, W.R., Scott, A., Hawthorne, F.C., Mertzman, S.A., 2008. Spectral reflectance properties of minerals exposed to simulated Mars surface conditions. Icarus 195, 140–168.
Cole, W.F., Lancucki, C.J., 1975. Huntite from Deer Park, Victoria, Australia. Am. Mineral. 60, 1130–1131.
Deer, W.A., Howie, R.A., Zussman, J., 1966. An Introduction to the Rock-Forming Minerals. Longman, Harlow, England. 528 pp.
Ehlmann, B., Mustard, J.F., Murchie, S.L., Poulet, F., Bishop, J.L., Brown, A.J., Calvin, W.M., Clark, R.N., Des Marais, D.J., Milliken, R.E., Roach, L.H., Roush, T.L., Swayze, G.A., Wray, J.J., 2008. Orbital identification of carbonate-bearing rocks on Mars. Science 322, 1828–1832.
Erard, S., 2001. A spectro-photometric model of Mars in the near-infrared. Geophys. Res. Lett. 28, 1291–1294.
Erard, S., Calvin, W., 1997. New composite spectra of Mars, 0.4–5.7 μm. Icarus 130, 449–460.
Farmer, V.C., 1974. The Infrared Spectra of Minerals. Mineralogical Society Monograph 4, London.
Fiorenza, C., Formisano, V., 2005. A solar spectrum for PFS data analysis. Planet. Space Sci. 53, 1009–1016.

Fonti, S., Jurewicz, A., Blanco, A., Blecka, M.I., Orofino, V., 2001. Presence and detection of carbonates on the martian surface. J. Geophys. Res. 106 (E11), 27815–27822.

Formisano, V., and 46 colleagues, 2005. The Planetary Fourier Spectrometer (PFS) onboard the European Mars Express mission. Planet. Space Sci. 53, 963–974.

Gaffey, S.J., McFadden, L.A., Nash, D., Pieters, C.M., 1993. Ultraviolet, visible, and near-infrared reflectance spectroscopy: Laboratory spectra of geologic materials. In: Pieters, C.M., Englert, P. (Eds.), Remote Geochemical Analysis: Elemental and Mineralogical Composition. Cambridge Univ. Press, New York, pp. 43–77.

Giuranna, M., and 20 colleagues, 2005a. Calibration of the Planetary Fourier Spectrometer short wavelength channel. Planet. Space Sci. 53, 975–991.

Giuranna, M., and 19 colleagues, 2005b. Calibration of the Planetary Fourier Spectrometer long wavelength channel. Planet. Space Sci. 53, 993–1007.

Grassi, D., Ignatiev, N.I., Zasova, L.V., Maturilli, A., Formisano, V., Bianchini, G.A., Giuranna, M., 2005. Methods for the analysis of data from the Planetary Fourier Spectrometer on the Mars Express Mission. Planet. Space Sci. 53, 1017–1034.

Halevy, I., Zuber, M.T., Schrag, D.P., 2007. A sulfur dioxide climate feedback on early Mars. Science 318, 1903–1907.

Hunt, G.R., 1982. Spectroscopic properties of rock and minerals. In: Carmichael, R.S. (Ed.), Handbook of Physical Properties of Rocks, vol. 1. CRC Press, Boca Raton, FL, pp. 295–385.

Kinsman, D.J.J., 1967. Huntite from a carbonate–evaporite environment. Am. Mineral. 52, 1332–1340.

Lane, M.D., Christensen, P.H., 1997. Thermal infrared emission spectroscopy of anhydrous carbonates. J. Geophys. Res. 102 (E11), 25581–25592.

Lane, M.D., Dyar, M.D., Bishop, J.L., 2004. Spectroscopic evidence for hydrous iron sulfate in the martian soil. Geophys. Res. Lett. 31, 19. CiteID L19702.

Lellouch, E., Encrenaz, T., de Graauw, T., Erard, S., Morris, P., Crovisier, J., Feuchtgruber, H., Girard, T., Burgdorf, M., 2000. The 2.4–45 μm spectrum of Mars observed with the infrared space observatory. Planet. Space Sci. 48, 1393–1405.

Orofino, V., Blanco, A., Fonti, S., Proce, R., Rotundi, A., 1998. The infrared optical constants of limestone particles and implications for the search of carbonates on Mars. Planet. Space Sci. 46, 1659–1669.

Pollack, J.B., Roush, T., Witteborn, F., Bregman, J., Wooden, D., Stoker, C., Toon, O.B., Rank, D., Dalton, B., Freedman, R., 1990. Thermal emission spectra of Mars (5.4–10.5 μm): Evidence for sulfates, carbonates, and hydrates. J. Geophys. Res. 95 (B9), 14595–14627.

Quinn, R., Zent, A.P., McKay, C.P., 2006. The photochemical stability of carbonates on Mars. Astrobiology 6, 581–591. doi:10.1089/ast.2006.6.581.

Salisbury, J.W., 1991. Infrared (2.1–25 μm) Spectra of Minerals. John Hopkins Univ. Press, Baltimore, MD, USA.

Salisbury, J.W., Wald, A., 1992. The role of volume scattering in reducing spectral contrast of reststrahlen bands in spectra of powdered minerals. Icarus 96, 121–128.

Smith, E., Gottlieb, D., 1974. Solar flux and its variations. Space Sci. Rev. 16, 771–802.

Stanger, G., Neal, C., 1994. The occurrence and chemistry of huntite from Oman. Chem. Geol. 112, 247–254.

Wagner, C., Schade, U., 1996. Measurements and calculations for estimating the spectrometric detection limit for carbonates in martian soil. Icarus 123, 256–268.

Wilson, S.A., Raudsepp, M., Dipple, G.M., 2006. Verifying and quantifying carbon fixation from serpentine-rich mine tailings using the Rietveld method with X-ray powder diffraction data. Am. Mineral. 91, 1331–1341.